Effects of D-Galactose on the Structure of Nerve Fibers in Cerebellar White Matter

Qingfeng Zhu, Xueping Ren and Changzheng Zhang*
School of Life Sciences, Anqing Normal University, 128 South Linghu Road, Anqing, Anhui 246011, China

Abstract.- Chronic administration of D-galactose (D-gal) has been widely reported to mimic brain aging, however, the potential mechanism underlying this phenomenon remains largely unclear. Here, we investigated whether and how the nerve fibers are altered by long-term D-gal exposure. After mice were treated with D-gal (100 mg/kg/day, s.c.) for 8 weeks, the cerebellar white matter was processed for transmission electron microscopy. The mean diameter of the myelinated fibers and axons, as well as the mean thickness of the myelin sheaths, was measured. The fiber diameter was 6.80% higher in the D-gal group compared with the controls ($P < 0.01$), with the peak diameter distribution shifting from1.0–1.2 μm in the control to 1.2–1.4 μm in the D-gal-treated group. Such an increase was principally due to the increase in the myelin sheath (19.43%) and less in the axon (6.68%). Myelin sheath thickening in D-gal-treated fibers may result from intra-myelin degeneration, such as loosening or splitting of the myelin lamellae, which ultimately alters the ratio of the sheath thickness to the fiber diameter. This is likely to impair impulse conduction velocity and play an important role in neural dysfunction in D-gal-treated animals.

Key words: Nerve fiber, myelin sheath, axon, cerebellar white matter; D-galactose

INTRODUCTION

It has been demonstrated that chronic administration of D-galactose (D-gal) is capable of causing morphological and functional impairments in the brain resembling symptoms of normal aging insults, and thus, it is considered an effective paradigm for establishing aging brain models (Cui *et al.*, 2006; Chen *et al.*, 2010; Park and Choi, 2012; Gu *et al.*, 2013). The neural impairments underlying the D-gal exposure are presumed to result from increased oxidative stress and disrupted neurotransmitter balance in nervous tissues (Cui *et al.*, 2006; Marosi *et al.*, 2012; Gu *et al.*, 2013). Intriguingly, a recent study reports that the number of neurons remains consistent in the cerebral cortex of animals with D-gal-induced aging (Gu *et al.*, 2013), and therefore, it is worthy of investigating whether the neuronal configurations undergo D-gal-dependent degeneration.

The nerve fibers are an important base for neural functioning. It is clear that myelin sheaths in nerve fibers in the normal aging brain exhibit marked degenerative alterations, such as forming splits and balloons (Bowley *et al.*, 2010; Peters and Kemper, 2012), which may correlate with the decline in nerve conduction velocity, and disruption in neuronal circuit timing (Lu *et al.*, 2013; Kemp *et al.*, 2014). The present study was designed to identify changes in the diameters of the myelinated fibers and axons, as well as the thickness of the myelin sheaths in the cerebellar white matter of control and chronic D-gal-treated mice. We sought to understand the influence of D-gal on the structures of nerve fibers, attempting to provide evidence for further investigations on mechanisms of chronic D-gal administration mimicking brain aging.

MATERIALS AND METHODS

Animals

Male Kunming mice (6 weeks of age, weighing 20±2 g) were randomly assigned into two groups: saline-treated group (0.9% saline, 1 ml/day s.c.; *n* = 4) and D-gal-induced aging group (D-gal, Sigma, St Louis, MO, USA, dissolved in 0.9% saline, 100 mg/ml/kg each day s.c.; *n* = 4); the treatment lasted for 6 consecutive weeks according to a well-established protocol (Prakash and Kumar, 2013; Hao *et al.*, 2014). Mice were individually raised in a temperature-controlled (22–24°C) and 12 h light/dark cycle, with food and water *ad libitum.*

Drug injection was performed at 16:00-17:00 h daily. All mice were monitored daily and weighed weekly in order to evaluate their health status. Animal housing and the experimental procedures were in accordance with the US National Institutes of Health Guide for the Care and Use of Laboratory Animals (NIH Publication 80-23, revised 1996).

Tissue preparation

Mice were anesthetized with sodium pentobarbital (Sigma; 40 mg/kg i.p.) and transcardially perfused with a solution of 2.5% glutaraldehyde and 4% paraformaldehyde in 0.1 M phosphate buffer (pH 7.4). The anterior cerebellum were collected and fixed with 3% glutaraldehyde in 0.1 M phosphate buffer overnight at 4°C. Four lobes containing the subcortical white matter were cut into pieces of around $1 \times 1 \times 1$mm, prior to fixation in 1% OsO_4 in 0.1 M sodium cacodylate buffer for 2 h at room temperature, and dehydration in an ascending acetone series. The osmicated tissue blocks were embedded in Epon-812 (Electron Microscopy Science, Hatfield, PA, USA) and trimmed under a light microscope. Semithick sections were first taken and stained with toluidine blue. The subcortical white matter was identified; then, the blocks were turned to obtain horizontal sections of the subcortical white matter, where the vertically oriented nerve fibers were arranged. Ultrathin sections (50–70 nm) were subsequently cut with a diamond knife on an LKB-11800 ultramicrotome (LKB, Stockholm, Sweden) and collected on 300-mesh copper grids. The ultrathin sections were stained with uranyl acetate and lead citrate and observed under an electron microscope (JEOL1400, Tokyo, Japan) and electron micrographs were captured at the same time.

Quantification of the fiber diameter, axon diameter and myelin sheath thickness

Electron micrographs were taken at a primary magnification of 10,000–100,000×, at which the myelin lamellae were distinct. For each block, the fiber diameter, axonal diameter and myelin sheath thickness were determined by at least 50 nerve fibers. The mean diameters of the fiber and axon were estimated according to our previously used formula (Zhang *et al.*, 2011a; Zhu *et al.*, 2011): d =

$(a \times b)^{1/2}$ (where a and b are the longitudinal and transversal diameters from the section, respectively). Each measurement was made three times and the mean values were taken as the values for a single fiber. All the measurements were made blind to the animal identity in order to avoid investigator bias.

The data were then arranged according to the fiber diameter of <0.4, 0.4–0.6, 0.6–0.8, 0.8–1.0, 1.0–1.2, 1.2–1.4, 1.4–1.6 and >1.6 µm in both the control and D-gal-treated groups. It should be noted that, as some fibers were sectioned obliquely, our quantitative measurements might be biased to an unknown degree due to the simply visual examination, thus, the measurements in this study were rough estimates. However, the results should not have been affected since the same criteria were used for both groups.

Quantitative analysis

The data are expressed as the mean ± SD. Student's *t* test and one-way analysis of variance followed by Fisher's Least Significant Difference post hoc test were used for statistical analysis. *P* values <0.05 were considered to be significant.

RESULTS

Compared with the control group, D-gal-treated mice developed mild dyskinesia and signs of slow reaction to various stimuli, which were consistent with other observations (Cui *et al.*, 2006; Gu *et al.*, 2013), indicating a successful D-gal-induced aging mouse model. The body weight showed a slight tendency to be elevated in the D-gal-treated mice when compared with these in the controls, but showed no statistical difference (data not shown).

Nerve fiber structure in D-gal-treated mice

Myelinated fibers from the control mice appeared compact and homogeneous with integral sheaths; whereas, the fibers from the D-gal-treated mice showed dilatation with irregular contours, in which some sheaths displayed obvious splitting and vacancy in some places (Fig. 1). Some sheaths appeared too loose for the enclosed axons, leaving a lot of space between the axon and myelin (Fig. 1).
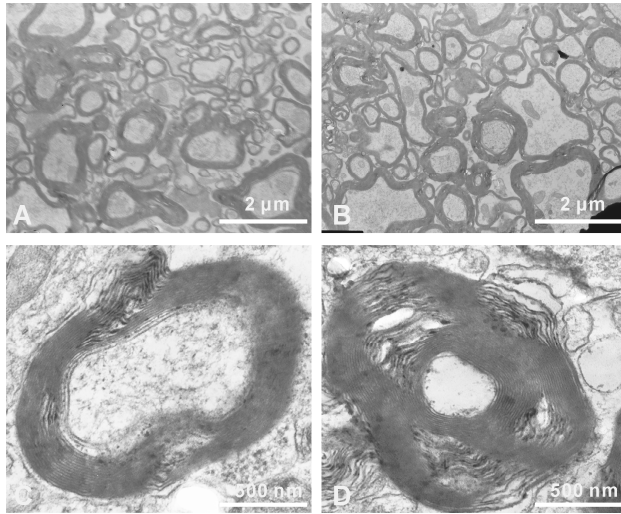
Fig. 1. Electron micrographs showing the myelinated fiber structures in cerebellar subcortical white matter from control (A, C) and D-gal-treated (B, D) mice.
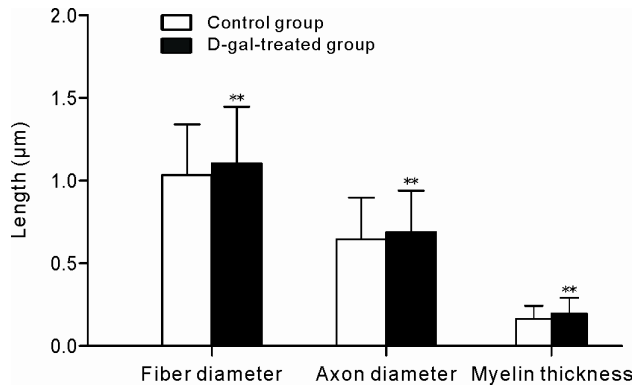
Fig. 2. Comparison of fiber diameter, axonal diameter and myelin sheath thickness between the control and D-gal-treated mice. **P <0.01 versus control.

Fig. 3. Comparison of the percentage distribution of the fiber diameters in control and D-gal-treated mice.
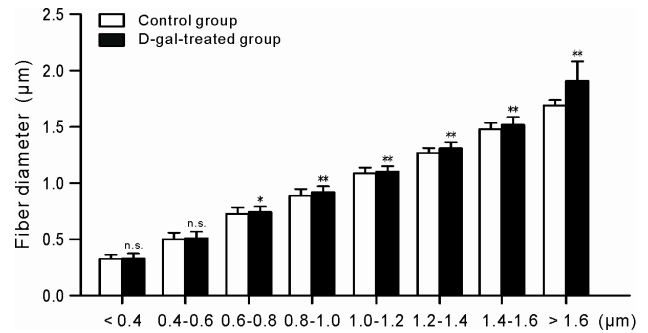
Fig. 4. The spectrum of fiber diameters in the control and D-gal-treated mice. n.s., no significance; *P <0.05; **P <0.01 versus control.

The fiber diameter ranged from 0.28 to 2.18 μm, however, the average fiber diameter in the D-gal-treated group was 1.10 μm, which was 6.80% thicker than that in the control group (1.03 μm). Such thickening might have been mainly due to the sheath thickness (19.43% increase) and less in the axon (only 6.68% increase) (P <0.01; Fig. 2), indicating that the myelin sheath underwent more severe alterations due to D-gal.

Fiber diameter, myelin sheath and axon diameter

To map the effects of D-gal on the structures of the specific fibers, we had a range of fiber diameters of <0.4, 0.4–0.6, 0.6–0.8, 0.8–1.0, 1.0–1.2 1.2–1.4, 1.4–1.6 and <1.6 μm (Fig. 3). Within-group analysis revealed that the fiber diameter was highly dependent on these segments [F(7,984) = 4995.341, P <0.01, in the control group; F(7,1051) = 4476.551, P <0.01, in the D-gal-treated group]. The peak fiber diameter distribution was 1.0–1.2 μm in the control group and shifted to 1.2–1.4 μm in the D-gal-treated mice. Compared with the controls, fiber diameters in the D-gal-treated mice showed no significant difference in the <0.4 and 0.4–0.6 μm segments (P >0.05), whereas they were increased by 4.38%, 6.54%, 5.60%, 6.36%, 5.28% and 13.02% in 0.6–0.8, 0.8–1.0, 1.0–1.2, 1.2–1.4, 1.4–1.6 and >1.6 μm segments, respectively (P <0.05 or 0.01; Fig. 4).
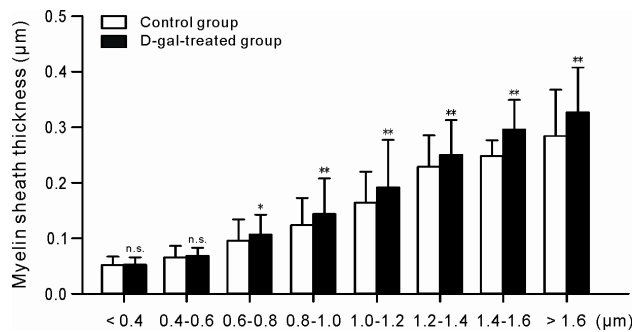
Fig. 5. Average thickness of the myelin sheaths in fibers of different diameter in the control and D-gal-treated mice. n.s., no significance; *P <0.05; **P <0.01 versus control.
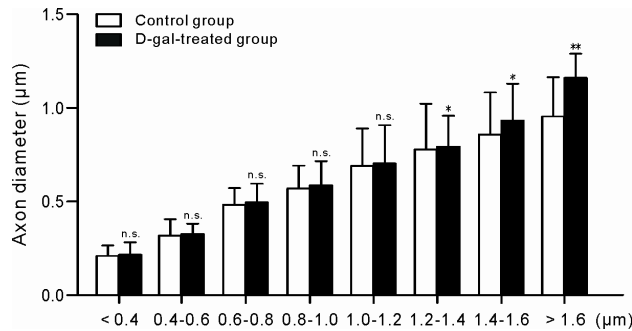
Fig. 6. Average diameter of the axons in fibers of different diameter in the control and D-gal-treated mice. n.s., no significance; *P <0.05; **P <0.01 versus control.

We analyzed alterations in the sheath thickness between the control and D-gal-treated mice based on the fiber diameter. Within-group analysis revealed that the sheath thickness was highly dependent on the diameter segments in both groups [F(7,984) = 205.444, P <0.01, in the control group; F(7,1051) = 206.235, P <0.01, in the D-gal-treated group]. Compared to the controls, a mean thickness of <0.4 and 0.4–0.6 μm showed no significant difference in the D-gal-treated mice (P <0.05), whereas the thickness significantly increased by 10.39%, 13.93%, 14.54%, 8.71%, 15.62% and 12.81% in 0.6–0.8, 0.8–1.0, 1.0–1.2 1.2–1.4, 1.4–1.6 and <1.6 μm segments, respectively (P <0.05 or 0.01; Fig. 5).

Finally, we investigated how D-gal affected the axonal diameter. In both the control and D-gal-treated mice, axonal diameter also showed a significant difference dependent on the fiber diameter [F(7,984) = 117.262, P <0.01, in the control group; F(7,1051) = 228.244, P <0.01, in the D-gal-treated group]. Compared to the control group, the mean thickness markedly increased only in the 1.4–1.6 and >1.6 μm segments (7.88% and 17.84%, respectively; P <0.01; Fig. 6) and showed no significant difference in other diameter segments in the D-gal-treated mice (P <0.05), indicating a weak increase in the axon due to D-gal exposure.

DISCUSSION

Several lines of evidence have demonstrated that chronic, systemic exposure to D-gal can induce acceleration of brain aging, and this paradigm has now been widely applied for establishing brain aging models (Cui *et al.*, 2006; Chen *et al.*, 2010; Park and Choi, 2012; Banji *et al.*, 2013; Gu *et al.*, 2013). It is reported that long-term treatment with D-gal induces many kinds of neurodegenerative symptoms, such as cognitive decline (Yu *et al.*, 2013; Zhou *et al.*, 2013; Stefanova *et al.*, 2014; Zhu *et al.*, 2014), deficits in learning and memory (Li *et al.*, 2012; Prisila-Dulcy *et al.*, 2012), and impaired locomotion (Banji *et al.*, 2013; Gu *et al.*, 2013). Potential contributing mechanisms may include induction of oxidative stress (Cui *et al.*, 2006; Banji *et al.*, 2013; Hao *et al.*, 2014; Zhu *et al.*, 2014), mitochondrial dysfunction (Prakash and Kumar, 2013), retrogression of neuronal organelles (Lei *et al.*, 2013), disruption in neurotransmitter balance (Gu *et al.*, 2013), and accumulation of β-amyloidprotein (Stefanova *et al.*, 2014). The results from our present study indicate that significant alterations also occur in the structures of nerve fibers.

From our observations, the myelinated nerve fibers from the D-gal-treated mice exhibited dilatation with irregular morphology, and the myelin lamellae were loosened with obvious splitting. These phenomena indicate chronic administration of D-gal caused marked degeneration of nerve fiber structures, which is in line with many reports in normal-aging fibers (Peters *et al.*, 2001; Peters, 2002), and correlates to our previous reported degenerations in cortical Purkinje cells (Zhang *et al.*, 2011b). We found that the dimensions of the fibers

appeared to increase in D-gal-treated mice compared with the controls, and this mainly resulted from an increase in the myelin sheath thickness. The increase in the myelin sheaths in D-gal-treated fibers may have been due to splitting and loosening of the myelin. In addition, as the demyelinated axons can be remyelinated (Fancy *et al*., 2011; Yang *et al*., 2013; Xie *et al*., 2014), we speculate that the mechanism underlying the myelin alterations in D-gal-treated animals is complicated, due to the concomitance of myelin breakdown and myelin re-formation.

In summary, our present study found that the fiber dimensions increased in D-gal-treated mice, which may have been mainly due to the increase in myelin sheath thickness. Such alterations may result in deficits in impulse conduction velocity and damage in neural circuits, which might be a potential mechanism for behavioral deficits produced by chronic D-gal administration.

ACKNOWLEDGEMENTS

Conflict of interest
The authors have no conflict of interest.

REFERENCES

BANJI, D., BANJI, O.J., DASAROJU, S. AND KRANTHI, K.C., 2013. Curcumin and piperine abrogate lipid and protein oxidation induced by D-galactose in rat brain. *Brain Res.,* **1515:** 1-11.

BOWLEY, M.P., CABRAL, H., ROSENE, D.L. AND PETERS, A., 2010. Age changes in myelinated nerve fibers of the cingulate bundle and corpus callosum in the rhesus monkey. *J. Comp. Neurol.,* **518:** 3046-3064.

CHEN, B., ZHONG, Y., PENG, W., SUN, Y. AND KONG, W.J., 2010. Age-related changes in the central auditory system: comparison of D-galactose-induced aging rats and naturally aging rats. *Brain Res.,* **1344:** 43-53.

CUI, X., ZUO, P., ZHANG, Q., LI, X., HU, Y., LONG, J., PACKER, L. AND LIU, J., 2006. Chronic systemic D-galactose exposure induces memory loss,

neurodegeneration and oxidative damage in mice: protective effects of R-alpha-lipoic acid. *J. Neurosci. Res.,* **83:** 1584-1590.

FANCY, S.P., CHAN, J.R., BARANZINI, S.E., FRANKLIN, R.J. AND ROWITCH, D.H., 2011. Myelin regeneration: a recapitulation of development? *Annu. Rev. Neurosci.,* **34:** 21-43.

GU, X., ZHOU, Y., HU, X., GU, Q., WU, X., CAO, M., KE, K. AND LIU, C., 2013. Reduced numbers of cortical GABA-immunoreactive neurons in the chronic d-galactose treatment model of brain aging. *Neurosci. Lett.,* **549:** 82-86.

HAO, L., HUANG, H., GAO, J., MARSHALL, C., CHEN, Y. AND XIAO, M., 2014. The influence of gender, age and treatment time on brain oxidative stress and memory impairment induced by D-galactose in mice. *Neurosci. Lett.,* **571:** 45-49.

KEMP, J., DESPRES, O., PEBAYLE, T. AND DUFOUR, A., 2014. Differences in age-related effects on myelinated and unmyelinated peripheral fibres: a sensitivity and evoked potentials study. *Eur. J. Pain,* **18:** 482-488.

LEI, M., ZHU, Z., WEN, Z. AND KE, S., 2013. Impairments of tight junctions are involved in D-galactose-induced brain aging. *Neuroreport,* **24:** 671-676.

LI, Z., ZHANG, Z., ZHANG, J., JIA, J., DING, J., LUO, R. AND LIU, Z., 2012. Cordyceps militaris extract attenuates D-galactose-induced memory impairment in mice. *J. Med. Food,* **15:** 1057-1063.

LU, P.H., LEE, G.J., TISHLER, T.A., MEGHPARA, M., THOMPSON, P.M. AND BARTZOKIS, G., 2013. Myelin breakdown mediates age-related slowing in cognitive processing speed in healthy elderly men. *Brain Cogn.,* **81:** 131-138.

MAROSI, K., BORI, Z., HART, N., SARGA, L., KOLTAI, E., RADAK, Z. AND NYAKAS, C., 2012. Long-term exercise treatment reduces oxidative stress in the hippocampus of aging rats. *Neuroscience,* **226:** 21-28.

PARK, J.H. AND CHOI, T.S., 2012. Polycystic ovary syndrome (PCOS)-like phenotypes in the d-galactose-induced aging mouse model. *Biochem. biophys. Res. Commun.,* **427:** 701-704.

PETERS, A., 2002. The effects of normal aging on myelin and nerve fibers: a review. *J. Neurocytol.,* **31:** 581-593.

PETERS, A. AND KEMPER, T., 2012. A review of the structural alterations in the cerebral hemispheres of the aging rhesus monkey. *Neurobiol. Aging,* **33:** 2357-2372.

PETERS, A., SETHARES, C. AND KILLIANY, R.J., 2001. Effects of age on the thickness of myelin sheaths in monkey primary visual cortex. *J. Comp. Neurol.,* **435:** 241-248.

PRAKASH, A. AND KUMAR, A., 2013. Pioglitazone alleviates the mitochondrial apoptotic pathway and mito-oxidative damage in the d-galactose-induced mouse model. *Clin. exp. Pharmacol. Physiol.,* **40:** 644-651.

PRISILA-DULCY, C., SINGH, H.K., PREETHI, J. AND RAJAN, K.E., 2012. Standardized extract of Bacopa monniera (BESEB CDRI-08) attenuates contextual associative learning deficits in the aging rat's brain induced by D-galactose. *J. Neurosci. Res.,* **90:** 2053-2064.

STEFANOVA, N.A., KOZHEVNIKOVA, O.S., VITOVTOV, A.O., MAKSIMOVA, K.Y., LOGVINOV, S.V., RUDNITSKAYA, E.A., KORBOLINA, E.E., MURALEVA, N.A. AND KOLOSOVA, N.G., 2014. Senescence-accelerated OXYS rats: a model of age-related cognitive decline with relevance to abnormalities in Alzheimer disease. *Cell Cycle,* **13:** 898-909.

XIE, F., LIANG, P., FU, H., ZHANG, J.C. AND CHEN, J., 2014. Effects of normal aging on myelin sheath ultrastructures in the somatic sensorimotor system of rats. *Mol. Med. Rep.,* **10:** 459-466.

YANG, S., LI, C., QIU, X., ZHANG, L., LU, W., CHEN, L., ZHAO, Y.Y., SHI, X.Y., HUANG, C.X., CHENG, G.H. AND TANG, Y., 2013. Effects of an enriched environment on myelin sheaths in the white matter of rats during normal aging: A stereological study. *Neuroscience,* **234:** 13-21.

YU, F., XU, B., SONG, C., JI, L. AND ZHANG, X., 2013. Treadmill exercise slows cognitive deficits in aging rats by antioxidation and inhibition of amyloid production. *Neuroreport,* **24:** 342-347.

ZHANG, C., ZHU, Q. AND HUA, T., 2011a. Age-related Increase in Astrocytes in the Visual Area V2 of the Cat. *Pakistan J. Zool.,* **43:** 777-780.

ZHANG, C., ZHU, Q. AND HUA, T., 2011b. Effects of ageing on dendritic arborizations, dendritic spines and somatic configurations of cerebellar Purkinje cells of old cat. *Pakistan J. Zool.,* **43:** 1191-1196.

ZHOU, Y., DONG, Y., XU, Q., HE, Y., TIAN, S., ZHU, S., ZHU, Y. AND DONG, X., 2013. Mussel oligopeptides ameliorate cognition deficit and attenuate brain senescence in D-galactose-induced aging mice. *Food Chem. Toxicol.,* **59:** 412-420.

ZHU, J., MU, X., ZENG, J., XU, C., LIU, J., ZHANG, M., LI, C., CHEN, J., LI, T. AND WANG, Y., 2014. Ginsenoside Rg1 prevents cognitive impairment and hippocampus senescence in a rat model of D-galactose-induced aging. *PLoS One,* **9:** e101291.

ZHU, Q., ZHANG, C. AND HUA, T., 2011. Ethanol induces a reduction in cortical thickness, neuronal density and somatic shrinkage in the cerebellar cortex of adult mice. *Neurochem. J.,* **5:** 133-137.